

# Asymmetries in oriented-line detection indicate two orthogonal filters in early vision

DAVID H. FOSTER AND PATRICK A. WARD

*Department of Communication and Neuroscience, University of Keele, Keele, Staffordshire ST5 5BG, U.K.*

## SUMMARY

Visual detection of a line target differing in orientation from a background of lines may be achieved speedily and effortlessly. Such performance is assumed to occur early in vision and to involve filter mechanisms acting in parallel over the visual field. This study establishes orientational limits on this performance and analytically derives some generic properties of the underlying filters. It was found that, in brief displays, target orientation detection thresholds increased approximately linearly with background orientation, from minima at 0° (vertical) and 90°, whereas background orientation detection thresholds decreased approximately linearly with target orientation, from maxima at 0° and 90°. Target and background threshold functions were exactly antisymmetric. These data are shown to indicate a model of early line processing dominated by two classes of orientation-sensitive filter with axes close to the vertical and horizontal and orientation-tuning half-widths each of approximately 30° at half-height.

## 1. INTRODUCTION

Detecting objects in a complex or cluttered visual scene is part of everyday visual experience. It is a task at which the visual system is adept and which has obvious evolutionary significance. There are several cues that determine detection performance, but in stationary, monochromatic images the orientation of edges and lines has a particular salience. Provided that a line-element 'target' differs in orientation from other line elements in a display, detection is fast and effortless (Beck & Ambler 1972; Sagi & Julesz 1985; Treisman 1985), as should be apparent from figure 1 (*a*).

Performance in this type of detection task is thought to be largely determined by the early stages of visual processing, sometimes referred to as *preattentive* (Neisser 1967; Treisman *et al.* 1977; Julesz 1981) or as involving *distributed* attention (Beck 1972). The fact that detection or search performance does not depend strongly on the number of background elements in the field has led to the notion that the underlying processing is essentially parallel (Treisman *et al.* 1977; Bergen & Julesz 1983; Javadian & Ruddock 1988; but see Sagi & Julesz (1987) and Duncan & Humphreys (1989)).

How the visual representation of the attributes extracted in the early processing of line elements differs from that when more focal attention is employed is not well understood at present. There is, however, a curious asymmetry in the detection of line targets in displays like those of figure 1, an asymmetry that is diagnostically useful. In figure 1 (*a*) the background lines are oriented vertically, and the tilted target is oriented at 15° to the vertical; in (*b*) the background lines are oriented at 15° to the vertical and the target is vertical. Detection, under appropriate viewing conditions, is easier in (*a*) than in (*b*).

Asymmetries of this kind have been reported in

visual search (Treisman & Souther 1985; Treisman & Gormican 1988; but see Sagi & Julesz (1987)) and in texture discrimination (Beck 1973, 1982; Gurnsey & Browse 1987; Rubenstein & Sagi 1990). One possible explanation for a search asymmetry with line elements is based on the notion that a tilted line element is coded as a vertical line with an additional feature marking the nature of the deviation (Treisman & Gormican 1988). The presence of the additional feature activity associated with the tilted element in a background of vertical elements, as in figure 1 (*a*), and its absence in (*b*), would account for the easier detection in (*a*). Another possible explanation assumes that visual filters responding to tilted elements are more noisy than those responding to vertical line elements (Rubenstein & Sagi 1990; but see Treisman & Gormican (1988)). Because the line elements in the background of figure 1 (*b*) are tilted and therefore generate a more noisy filtered image than when they are vertical, the target would be easier to detect in (*a*).

Neither explanation of search asymmetries has been developed quantitatively, although computational models have been implemented for asymmetries in texture segmentation (Gurnsey & Browse 1989; Rubenstein & Sagi 1990). No systematic data are available on orientation thresholds for detection in multi-element displays, despite an abundant literature on orientation effects in sparse displays (see, for example, Appelle (1972) and Essock (1980) for reviews). Apart from a few studies (e.g. those of Ike *et al.* (1987) and Alkhateeb *et al.* (1990)) the choice of stimulus orientations in search and detection tasks has been restricted to three or four, usually including the vertical and horizontal. Additionally, response time has generally been the dependent variable, rather than some criterion-free measure of visual detection performance.

In this study, signal-detection-theoretic measures of

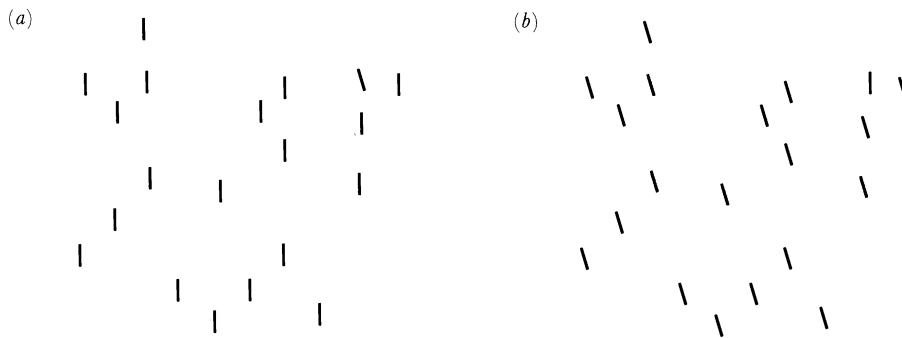


Figure 1. Demonstration of an asymmetry in the detection of oriented lines. In (a) the background lines are oriented vertically, and the 'target' line is oriented at  $15^\circ$  to the vertical. In (b) the target and background orientations are reversed.

detection performance were used to determine, parametrically, orientation thresholds for changes in target and background line-element orientations in brief displays. An analysis of possible detection schemes is shown to indicate a model of early line processing dominated by two classes of broad-band orientation-sensitive filters, the tuning characteristics of which may be estimated by integration of the orientation-threshold functions.

## 2. DETECTING ORIENTED LINE TARGETS

The experiment determined angular thresholds for the detection of a target in multi-element fields, of the kind illustrated in figure 1 (in reverse contrast). The stimulus display consisted of twenty identical white line elements distributed randomly over the  $20^\circ \times 20^\circ$  field. Each line subtended  $1^\circ$ , with width approx.  $0.1^\circ$ . All the line elements in the display had the same orientation except for the target, which was presented with probability of 0.5 in each trial. (The 'non-target' displays had the same number of elements as the target displays.) The orientation of the target and its spatial location within an annulus of radius  $3^\circ$ – $8^\circ$ , and the orientation of the background elements and their spatial locations, were all chosen randomly (within minor constraints). The stimulus display was followed by an interstimulus interval (ISI) consisting of a blank field, and then a post-stimulus mask, which controlled the time available for inspection of the afterimage. The mask consisted of twenty patches of four randomly oriented lines, each patch covering one of the previously displayed line elements.

Stimuli were presented with a cathode-ray-tube (CRT) display (Hewlett-Packard, Type 1321A, white P4 sulfide phosphor) controlled by a vector-graphics generator (Sigma Electronic Systems, QVEC 2150) and additional digital-to-analogue converters (DACs), in turn controlled by a 16-bit laboratory computer (details in Foster & Ferraro (1989)). This system produced very high-resolution line-element displays in which individual line elements were defined with end-point (linear) resolutions of 1 part in 1024 over a square 'patch' of side approximately 1 cm. Each patch was located with a precision of 1 part in 4096 over the CRT screen. Because a vector-graphics system was employed, aliasing artifacts, sometimes associated with

raster-graphics displays, were absent. The display was refreshed at intervals of 20 ms. (This temporal structure was not visually detectable.) Subjects viewed the display binocularly at 50 cm through a view-tunnel, which produced a uniformly illuminated, white background, luminance  $50 \text{ cd m}^{-2}$ , on which the stimuli appeared superimposed. Stimulus luminance was set by each subject at the beginning of each experimental session to 1  $\log_{10}$  unit above increment threshold.

On the basis of preliminary experiments, the stimulus duration was fixed at 40 ms, the ISI at 60 ms, and the mask duration at 500 ms. Subjects initiated each trial and signalled their response as to whether a target was present by using two push-button boxes connected to the computer. Fresh random displays were generated in every trial. The ordering of testing target- and background-orientation combinations was chosen randomly and conditions were not blocked. Data were obtained from ten subjects. They each had normal or corrected-to-normal vision (Snellen acuity at least 6/6, without astigmatism), were aged 19–24 years, and were unaware of the purpose of the experiment. In all they performed approximately 43000 trials.

Detection performance for each combination of target and background orientations was summarized by the discrimination index  $d'$  from signal detection theory (Green & Swets 1966). The index  $d'$  is zero when performance is at chance level and increases monotonically with improvement in performance. This index has a number of advantages as a measure of detection performance (Swets 1973), including additivity and freedom from bias (Durlach & Braida 1969). No significant difference was found between computing  $d'$  from pooled 'hit' and 'false-alarm' scores and as an average over individual  $d'$  values ( $\chi^2(136) = 79, p > 0.5$ ). The pooled values were used.

Plots of target detection  $d'$  were obtained as a function of the difference  $\Delta\theta = 10^\circ, 20^\circ, \dots, 170^\circ$  between target orientation and background orientation for target orientations of  $\theta = 0^\circ, 22.5^\circ, \dots, 157.5^\circ$  ( $0^\circ$  vertical, positive anticlockwise). Some of the detection functions showed changes in concavity with  $\Delta\theta$ , and therefore cubic curves were fitted to the data, by a method of least squares. For a selected criterion value of  $d'$ , the corresponding background incremental and decremental thresholds  $\Delta\theta$  were then computed for

each target orientation  $\theta$ . The standard deviation of each such threshold was estimated by a bootstrap procedure (Foster & Bischof 1987). An analogous set of target thresholds was obtained for  $d'$  as a function of the difference between background orientation and target orientation for *background* orientations of  $\theta = 0^\circ, 22.5^\circ, \dots, 157.5^\circ$ . Both target and background thresholds were symmetric with respect to reversal in the sign of  $\theta$  and  $\Delta\theta$  ( $\chi^2(8) \leq 7.7, p > 0.2$ ), and thresholds were averaged over these two conditions.

The choice of criterion values of  $d'$  was not determined by their absolute values, which depended on stimulus time course, but on the properties of the derived thresholds. There were two requirements: the stability of the threshold estimates (i.e. small standard deviations), and the invariance of the form of the threshold functions ( $\Delta\theta$  against  $\theta$ ) under reasonable changes in  $d'$ . Although actual values of  $d'$  achieved by subjects exceeded 1.0, criterion values of 0.8 and larger failed one or both of these requirements.

Figure 2 shows (a) target incremental threshold  $\Delta\theta$  against background orientation  $\theta$ , and (b) background incremental threshold  $\Delta\theta$  against target orientation  $\theta$ , for criterion values of  $d' = 0.2, 0.5$ . Even for these modest  $d'$  values, thresholds varied from  $5^\circ$  to  $31^\circ$ , with approximately linear dependencies over the ranges  $0^\circ$  to  $67.5^\circ$  and  $90^\circ$  to  $157.5^\circ$ . The form of the threshold functions was evidently stable under these  $d'$  values.

Target and background threshold functions were exact inverses of each other: target thresholds were minimum at background orientations of  $0^\circ$  and  $90^\circ$ , and maximum at  $67.5^\circ$  and  $157.5^\circ$ , and background thresholds were maximum at target orientations of  $0^\circ$  and  $90^\circ$ , and minimum at  $67.5^\circ$  and  $157.5^\circ$ . (The discontinuities in performance near  $90^\circ$  and  $180^\circ$  make more precise estimates uncertain.) Notice that the asymmetries in the threshold functions about  $0^\circ$  and  $90^\circ$  do not imply that the underlying visual mechanisms are asymmetric about the vertical and

horizontal. Consider, for example, a target with orientation  $\Delta\theta = 22.5^\circ$  relative to backgrounds with orientations  $\theta = 67.5^\circ, 112.5^\circ$ . Although the background orientations are symmetric about  $90^\circ$ , and ought to yield similar responses, the absolute target orientations  $\theta + \Delta\theta = 90^\circ, 135^\circ$  are *not* symmetric about  $90^\circ$ , and ought, in general, to yield different responses.

These patterns of anisotropic performance are incompatible with an interpretation based on the classical oblique effect (Appelle 1972; Essock 1980), which would simply predict minima at  $0^\circ$  and  $90^\circ$ , and maxima at  $45^\circ$  and  $135^\circ$ , for both target and background threshold functions. The antisymmetry of the target and background threshold functions provides a generalization of the search-time data obtained by Treisman & Gormican (1988) for target and background orientations close to the vertical, given the assumption of a monotonic relationship between discrimination performance and response time.

There is a superficial analogy between these measurements and the measurements made by Stiles (1978) on test and field spectral sensitivities of the colour mechanisms of the human eye. In test spectra determinations, the threshold intensity of a test flash is determined as a function of its wavelength; in field spectra determinations, the threshold intensity of a background that has a criterion effect on the test flash (of fixed wavelength and intensity) is determined as a function of the background wavelength. If test and field spectra coincide, then a common, unitary mechanism is argued to underlie both (Stiles 1978).

A similar argument applied here would imply that there is more than one orientation-sensitive mechanism underlying the target and background orientation-threshold functions of figure 2. In the next section, it is shown that *two* orientation-sensitive mechanisms are necessary and sufficient.

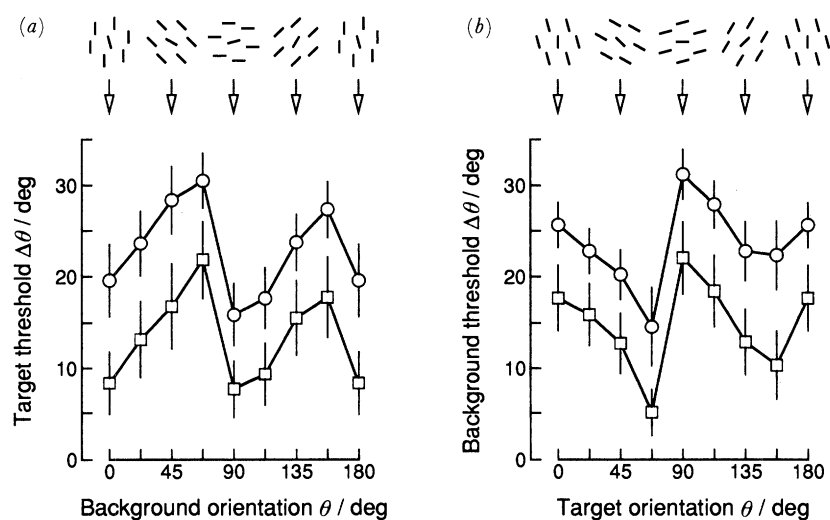


Figure 2. Incremental detection threshold functions. (a) Threshold difference angle  $\Delta\theta$  between target-element orientation and background-element orientation as a function of background-element orientation  $\theta$ ; (b) threshold difference angle  $\Delta\theta$  between background-element orientation and target-element orientation as a function of target-element orientation  $\theta$  ( $0^\circ$  vertical, positive anticlockwise). Circle and square symbols refer to detection criteria of  $d' = 0.5$  and  $0.2$  respectively. The ikons above indicate the display configuration; see figure 1. (Vertical bars,  $\pm 1$  s.e.m.; data from 10 subjects.)

### 3. TWO ORTHOGONAL ORIENTATION-SENSITIVE FILTERS

Consider the general case of a population of local line-sensitive filter units distributed over the visual field, the units parametrized by their 'preferred' orientations  $\phi$ . Thus, if  $f(\theta, \phi)$  is the response of a unit to an appropriately located line element of orientation  $\theta$ , then  $f(\theta, \phi)$  is maximum at  $\theta = \phi$ . (Other factors determining the unit's response such as element line length and intensity are irrelevant here.) The response  $r_{\text{non-tar}}$  of a subpopulation of such units with a particular preferred orientation  $\phi$  to a non-target array of  $n$  line elements of identical orientation  $\theta$  may be assumed to be of the form  $r_{\text{non-tar}} = nf(\theta, \phi)$ , or scaled by some monotonic function of  $n$ ; more definite assumptions about probability summation and the like are unnecessary. The response  $r_{\text{tar}}$  of this subpopulation of units to a target array of  $n-1$  line elements of orientation  $\theta$  and one line element (the target element) of absolute orientation  $\theta + \Delta\theta$  may then be assumed to be of the form

$$r_{\text{tar}} = (n-1)f(\theta, \phi) + f(\theta + \Delta\theta, \phi).$$

Observed detection, that is the value of  $d'$ , will depend on the ratio of  $r_{\text{tar}}$  to  $r_{\text{non-tar}}$ , maximized over all filter-unit preferred orientations  $\phi$ . A ratio is a more appropriate comparison than a difference, for the latter, being independent of  $n$  for all  $n \geq 1$ , yields results indistinguishable from those for a single-element display. Thus, for a given level of performance  $d'$  and background orientation  $\theta$ ,

$$\max_{\phi} \left\{ \frac{(n-1)f(\theta, \phi) + f(\theta + \Delta\theta, \phi)}{nf(\theta, \phi)} \right\} = c, \quad (1)$$

where the constant  $c$  depends on  $d'$ . The value of  $\Delta\theta$  that satisfies equation 1 is the target incremental threshold at that value of  $\theta$ .

How then do variations in  $\Delta\theta$  with  $\theta$  arise? Suppose that for each preferred orientation  $\phi$  the tuning curve of the filter, that is the variation of  $f(\theta, \phi)$  with  $\theta$ , is of some smooth generic form, symmetric about  $\theta = \phi$ , of variable height and width, and such that  $\partial f(\theta, \phi) / \partial \theta = 0$  at  $\theta = \phi, \phi \pm \tau$ , for fixed  $\tau$ , with  $0^\circ < \tau \leq 90^\circ$ . A variety of psychophysically and physiologically plausible local image operators will yield such orientation-tuning functions. For a filter with preferred orientation  $\phi$ , let  $f_{\text{max}}(\phi)$  be the maximum value of  $f(\theta, \phi)$  over  $\theta$ , that is,  $f_{\text{max}}(\phi) = \max_{\theta} \{f(\theta, \phi)\}$ , and let  $\sigma(\phi)$  be the orientation half-width at half-height, that is  $f(\phi + \sigma(\phi), \phi) = 0.5f(\phi, \phi)$ .

Any model of detection performance has to account for (i) the progressive increase in incremental threshold  $\Delta\theta$  with  $\theta$  from  $\theta = 0^\circ$  and from  $\theta = 90^\circ$  in the target-threshold data, (ii) the asymmetry in target incremental thresholds about  $\theta = 0^\circ$  and  $\theta = 90^\circ$ , and (iii) the antisymmetry of target and background incremental threshold functions (figure 2). At least three types of distribution of filters  $f(\theta, \phi)$  may be distinguished, based on preferred orientations  $\phi$  and half-widths  $\sigma(\phi)$ .

Model 1:  $\phi$  and  $\sigma(\phi)$  vary continuously; per-

formance anisotropies result from (smooth) variations in the size of  $\sigma(\phi)$  with  $\phi$ ,  $\sigma(\phi)$  being minimum at  $\phi = 0^\circ, 90^\circ$ , and varying approximately symmetrically about those axes (Andrews 1967).

Model 2:  $\phi$  varies continuously, but  $\sigma(\phi)$  is constant; performance anisotropies result from (smooth) variations in the size of  $f_{\text{max}}(\phi)$  with  $\phi$ ,  $f_{\text{max}}(\phi)$  being maximum at  $\phi = 0^\circ, 90^\circ$  and varying approximately symmetrically about those axes (models in which the density of filter units varies with  $\phi$  are merged with this model) (Bouma & Andriessen 1968).

Model 3:  $\phi$  varies discretely, with at least two values,  $\phi = 0^\circ, 90^\circ$ ; performance anisotropies result from variations in the value of  $f(\theta, \phi)$  with  $\theta$ .

Consider Model 1. Let  $\Delta\theta_1$  and  $\Delta\theta_2$  be the incremental thresholds at  $\theta_1$  and  $\theta_2$  respectively, and suppose  $0^\circ < \theta_1 < \theta_2 \leq 90^\circ$ . The effect of changing  $\theta$  in equation 1 is approximately equivalent to a local rescaling of  $\phi$  according to the half-width  $\sigma(\phi)$ . That is, for any  $f(\theta, \phi)$ , there exists  $\phi'$  such that  $f(\theta_1, \phi) = f(\theta_2, \phi')$  and  $f(\theta_1 + \Delta\theta_1, \phi) = f(\theta_2 + \Delta\theta_2, \phi')$ . Since  $\Delta\theta_2 = \Delta\theta_1 \cdot \sigma(\phi') / \sigma(\phi)$  and  $\sigma(\phi) < \sigma(\phi')$ , it follows that  $\Delta\theta_1 < \Delta\theta_2$ . Incremental thresholds therefore increase with  $\theta$  from  $\theta = 0^\circ$ , as observed in figure 2(a). An analogous argument applies for orientations close to  $90^\circ$ .

Now test for asymmetry in target incremental thresholds about  $\theta = 0^\circ$ . Let  $\Delta\theta'_1$  be the corresponding decremental threshold at  $\theta_1$ , that is the value of  $\Delta\theta$  in equation 1 in which  $f(\theta + \Delta\theta, \phi)$  is replaced by  $f(\theta - \Delta\theta, \phi)$ . Suppose that  $\Delta\theta'_1 < \theta_1 < \theta_2 \leq 90^\circ$ . Because of the smooth variation in  $\sigma(\phi)$  with  $\phi$ , it follows that, for small  $d'$  and therefore small  $\Delta\theta_1$ ,  $\Delta\theta'_1$  is approximately equal to  $\Delta\theta_1$ . But this is in contradiction with the data of figure 2(a), for  $\Delta\theta'_1 = \Delta\theta_1$  at  $\theta = -\theta_1$  by the previously noted symmetry in thresholds under sign reversal, and it is evident from figure 2(a) that  $\Delta\theta$  at small negative values of  $\theta$  (equivalently close to but less than  $180^\circ$ ) is much greater than  $\Delta\theta$  at small positive values of  $\theta$ .

Next consider Model 2. The effects of variations in  $f_{\text{max}}(\phi)$  with  $\phi$  are eliminated in equation 1, and the model fails to predict any orientational anisotropies. If a more complex combination of  $r_{\text{tar}}$  and  $r_{\text{non-tar}}$  is contrived, then a similar argument to that used for Model 1 shows that incremental and decremental values of  $\Delta\theta$  should be approximately equal, again in contradiction to the data of figure 2(a).

Finally consider Model 3. Take the smallest possible number of values of  $\phi$ , namely  $\phi = 0^\circ, 90^\circ$ . Over the range  $0^\circ \leq \theta < 90^\circ - \Delta\theta$ , the ratio

$$f(\theta + \Delta\theta, 90^\circ) / f(\theta, 90^\circ) > 1,$$

since  $f(\theta, 90^\circ)$  is increasing with  $\theta$ , and the ratio  $f(\theta + \Delta\theta, 0^\circ) / f(\theta, 0^\circ) < 1$ , since  $f(\theta, 0^\circ)$  is decreasing with  $\theta$ . Hence equation 1 reduces to

$$\frac{(n-1)f(\theta, 90^\circ) + f(\theta + \Delta\theta, 90^\circ)}{nf(\theta, 90^\circ)} = c. \quad (2)$$

This equation also holds over the range

$-90^\circ + \Delta\theta < \theta \leq 0^\circ$ , for decremental thresholds  $\Delta\theta$ . Analogously, over the range  $90^\circ \leq \theta < 180^\circ - \Delta\theta$  (and over the range  $\Delta\theta < \theta \leq 90^\circ$  for decremental thresholds  $\Delta\theta$ ), equation 1 reduces to

$$\frac{(n-1)f(\theta, 0^\circ) + f(\theta + \Delta\theta, 0^\circ)}{nf(\theta, 0^\circ)} = c. \quad (3)$$

Thus, the 'horizontal' filter  $f_h(\theta) = f(\theta, 90^\circ)$  determines performance over the interval  $0^\circ \leq \theta < 90^\circ - \Delta\theta$  for increments  $\Delta\theta$ , and over  $-90^\circ + \Delta\theta < \theta \leq 0^\circ$  for decrements (equation 2), and the 'vertical' filter  $f_v(\theta) = f(\theta, 0^\circ)$  determines performance over the interval  $90^\circ \leq \theta < 180^\circ - \Delta\theta$  for increments, and over  $\Delta\theta < \theta \leq 90^\circ$  for decrements (equation 3).

Now test for an increase in target incremental thresholds with  $\theta$ . Again let  $\Delta\theta_1$  and  $\Delta\theta_2$  be the incremental thresholds at  $\theta_1$  and  $\theta_2$  respectively, with  $0^\circ < \theta_1 < \theta_2 \leq 90^\circ$ . If  $f_h(\theta)$  does not increase too rapidly with  $\theta$  (an estimate is made later), the ratio

$$f_h(\theta_1 + \Delta\theta_1)/f_h(\theta_1) > f_h(\theta_2 + \Delta\theta_1)/f_h(\theta_2).$$

Hence,  $\Delta\theta_1 < \Delta\theta_2$ , and incremental thresholds increase with  $\theta$  from  $\theta = 0^\circ$ , as observed in figure 2(a). An analogous argument applies over the interval  $90^\circ \leq \theta < 180^\circ - \Delta\theta$  for  $f_v(\theta)$ .

Next test for asymmetry in target incremental thresholds about  $\theta = 0^\circ$ . Let  $\Delta\theta'_1$  be the corresponding decremental threshold at  $\theta_1$ , with  $\Delta\theta'_1 < \theta_1 < \theta_2 \leq 90^\circ$ . Then equation 3 applies. But as the ratio

$$f_v(\theta_1 - \Delta\theta'_1)/f_v(\theta_1) \ll f_h(\theta_1 + \Delta\theta_1)/f_h(\theta_1)$$

( $f_v(\theta_1)$  is close to maximum,  $f_h(\theta_1)$  is close to zero), the decremental threshold  $\Delta\theta'_1 \gg \Delta\theta_1$ , and as  $\Delta\theta'_1$  is equivalent to an incremental threshold at  $\theta = -\theta_1$ , it follows that  $\Delta\theta$  at small negative values of  $\theta$  (equivalently close to but less than  $180^\circ$ ) is much greater than  $\Delta\theta$  at small positive values of  $\theta$ . This is consistent with the observed asymmetry about  $\theta = 0^\circ$  in figure 2(a). An analogous argument applies for orientations  $\theta_1, \theta_2$  close to  $90^\circ$ .

Finally test for antisymmetry of target and background incremental threshold functions. Consider equation 1 again. For background incremental thresholds, exchange  $\theta$  and  $\theta + \Delta\theta$ . Over the range  $0^\circ \leq \theta < 90^\circ - \Delta\theta$ , the ratio  $f_v(\theta)/f_v(\theta + \Delta\theta) > 1$  and the ratio  $f_h(\theta)/f_h(\theta + \Delta\theta) < 1$ , and performance is determined by the vertical filter  $f_v$ . Let  $\Delta\theta_1$  and  $\Delta\theta_2$  be the background incremental thresholds at  $\theta_1$  and  $\theta_2$  respectively, with  $0^\circ < \theta_1 < \theta_2 \leq 90^\circ$ . Provided that  $f_v(\theta)$  does not decrease too rapidly with  $\theta$  (again an estimate is made later), the ratio

$$f_v(\theta_1)/f_v(\theta_1 + \Delta\theta_1) < f_v(\theta_2)/f_v(\theta_2 + \Delta\theta_1).$$

Hence,  $\Delta\theta_1 > \Delta\theta_2$ , that is, background incremental thresholds decrease with  $\theta$ , as observed in figure 2(b). An analogous argument applies for  $f_h(\theta)$  over the interval  $90^\circ \leq \theta < 180^\circ - \Delta\theta$ .

Note that in Model 3 if, say,  $\phi = 90^\circ$  were replaced by  $\phi = \phi'$ , with  $0^\circ < \phi' < 90^\circ$ , then a minimum in  $\Delta\theta$  at  $\theta = 0^\circ$  would imply a minimum in  $\Delta\theta$  at  $\theta = 2\phi'$ , which is possible only if  $\phi' = 45^\circ$ . That, in turn, would imply a maximum in  $\Delta\theta$  at or near  $\theta = 45^\circ$ , because

$f_v(\theta)$  is decreasing with  $\theta$ , and there is no evidence of such a maximum in figure 2(a).

#### 4. FILTER TUNING CURVES

The incremental-threshold data of figure 2 may be used to make an estimate of the tuning curves of the vertical and horizontal filters,  $f_v$  and  $f_h$ . Let  $f$  stand for either  $f_v$  or  $f_h$ . Make a Taylor's series expansion of  $f(\theta + \Delta\theta)$  about  $\theta$ . For  $\Delta\theta$  sufficiently small relative to  $\theta$ , equations 2 and 3 take the form

$$\frac{df(\theta)/d\theta \cdot \Delta\theta}{f(\theta)} = c', \quad (4)$$

where  $c'$  is constant. Let the variation of the incremental threshold  $\Delta\theta$  with  $\theta$  over the appropriate range be denoted by  $g$ . Then equation 4 may be rewritten as

$$\frac{df}{f} = \frac{d\theta}{g} \cdot c',$$

which, after integration, yields

$$f(\theta) = a \exp\left(b \int g^{-1} d\theta\right), \quad (5)$$

where  $a$  and  $b$  are constants, to be established separately for  $f = f_v, f_h$ .

Figure 3 shows the results of evaluating equation 5 for the threshold data of figure 2(a), with  $d' = 0.5$ . The appropriate thresholds for positive- and negative-going  $\theta$  rather than their averages were used so that a full  $180^\circ$  range could be fitted. As line elements of orientation  $\theta$  and  $\theta + 180^\circ$  are indistinguishable, plots were not extended beyond  $180^\circ$  ranges. The smooth curves (each of which has three degrees of freedom) are best-fitting Gaussians, and both account well for the variance in the data ( $\chi^2(5) \leq 6.2, p > 0.2$ ). In fact, a

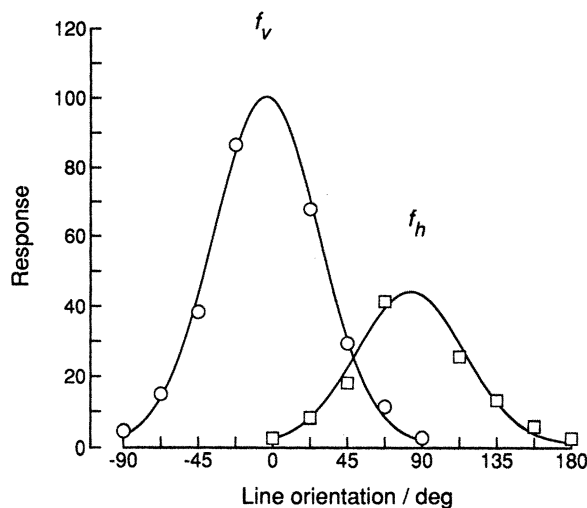


Figure 3. Estimated filter functions. Circle and square symbols are the result of numerically integrating equation 5 to define vertical and horizontal filters  $f_v$  and  $f_h$  respectively. The smooth curves are best-fitting Gaussians with midpoints  $-4^\circ \pm 8^\circ$  and  $83^\circ \pm 6^\circ$  and half-widths  $31^\circ \pm 3^\circ$  and  $32^\circ \pm 3^\circ$  respectively, computed with a bootstrap procedure (Foster & Bischof 1987). Because line elements with orientations of  $\theta$  and  $\theta + 180^\circ$  are indistinguishable, the functions are shown only over  $180^\circ$  ranges.

piecewise power-law function provides a slightly better fit, evaluated by predicting thresholds from the estimated filter functions. Over most of the range, however, the Gaussian and piecewise power-law functions are indistinguishable.

The half-widths of the vertical and horizontal filters in figure 3 were determined as 31° and 32° respectively. These values fall within the 20°–40° range estimated by Alkhateeb *et al.* (1990) for channel tuning half-widths underlying search-time performance with single line-element targets in line-element backgrounds with two orientations. The maximum response of the vertical filter in figure 3 was greater than that of the horizontal filter by a factor of 2.3. This asymmetry of vertical and horizontal responses parallels that in detection and discrimination tasks requiring explicit judgements of pattern symmetry (Palmer & Hemenway 1978; Barlow & Reeves 1979).

## 5. COMMENT

The most notable feature of this analysis is the implication that two broad-band orientation-sensitive filters are necessary and sufficient to explain line-orientation detection dependencies in early vision. In contrast, orientation data obtained in psychophysical experiments with simple, long-duration, and centrally fixated stimuli show narrower bandwidths and essentially continuous distributions of preferred orientations (Campbell & Kulikowski 1966; Blakemore & Nachmias 1971; Thomas & Gille, 1979; Regan & Beverley 1985). But this type of dichotomy is not novel: it has been observed in other spatial judgement tasks involving distributed and focal attention, and a variety of explanatory processes have been proposed ranging from low-level differences in response times to more central 'resource-constraint bottlenecks' (see, for example, Beck & Ambler 1972; Foster 1983; Watt 1987; Foster & Ferraro 1989). The reduction to two in the effective number of classes of processing mechanisms has also been observed before, in discriminating brief displays containing lines differing in collinearity and in continuity (Foster & Ferraro 1989).

Any comparison of the present orientation-tuning data with those from single-cell recordings from the visual cortex is difficult because of the disparity in experimental conditions and the great variety in recorded responses, even from a single category of cell (Hubel & Wiesel 1968; Campbell *et al.* 1968; Rose & Blakemore 1974; Kennedy *et al.* 1985). The two classes of filter derived here may represent either the two most active classes of cortical cell or some pooled activity of cortical cells mediating early visual processing. The issue is certainly more complicated, however, for what constitutes the vertical in detection experiments of the present kind may be influenced by the display environment (Treisman & Gormican 1988; Marendaz & Stivalet 1990) as well as by anisotropies in the retina and cortex.

We are grateful to G. W. Humphreys, I. R. Moorhead, K. H. Ruddock, D. Sagi, D. R. Simmons, A. Treisman, and S. Westland for critical review of a preliminary version of this paper. This work was supported by the Procurement

Executive of the Ministry of Defence under contract number D/ER1/9/4/2098/007.

## REFERENCES

- Alkhateeb, W., Morris, R. J. & Ruddock, K. H. 1990 Effects of stimulus complexity on simple spatial discriminations. *Spatial Vis.* **5**, 129–141.
- Andrews, D. P. 1967 Perception of contour orientation in the central fovea. Part 1: Short lines. *Vision Res.* **7**, 975–997.
- Appelle, S. 1972 Perception and discrimination as a function of stimulus orientation: The 'oblique effect' in man and animals. *Psychol. Bull.* **78**, 266–278.
- Barlow, H. B. & Reeves, B. C. 1979 The versatility and absolute efficiency of detecting mirror symmetry in random dot displays. *Vision Res.* **19**, 783–793.
- Beck, J. 1972 Similarity grouping and peripheral discriminability under uncertainty. *Am. J. Psychol.* **85**, 1–19.
- Beck, J. 1973 Similarity grouping of curves. *Percept. Motor Skills* **36**, 1331–1341.
- Beck, J. 1982 Textural segmentation. In *Organization and representation in perception* (ed. J. Beck), chapter 15, pp. 285–317. Hillsdale, New Jersey: Lawrence Erlbaum Associates.
- Beck, J. & Ambler, B. 1972 Discriminability of differences in line slope and in line arrangement as a function of mask delay. *Percept. Psychophys.* **12**, 33–38.
- Bergen, J. R. & Julesz, B. 1983 Parallel versus serial processing in rapid pattern discrimination. *Nature, Lond.* **303**, 696–698.
- Blakemore, C. & Nachmias, J. 1971 The orientational specificity of two visual after-effects. *J. Physiol.* **213**, 157–174.
- Bouma, H. & Andriessen, J. J. 1968 Perceived orientation of isolated line segments. *Vision Res.* **8**, 493–507.
- Campbell, F. W., Cleland, B. G., Cooper, G. F. & Enroth-Cugell, C. 1968 The angular selectivity of visual cortical cells to moving gratings. *J. Physiol.* **198**, 237–250.
- Campbell, F. W. & Kulikowski, J. J. 1966 Orientational selectivity of the human visual system. *J. Physiol.* **187**, 437–445.
- Duncan, J. & Humphreys, G. W. 1989 Visual search and stimulus similarity. *Psychol. Rev.* **96**, 433–458.
- Durlach, N. I. & Braida, L. D. 1969 Intensity perception. I. Preliminary theory of intensity resolution. *J. acoust. Soc. Am.* **46**, 372–383.
- Essock, E. A. 1980 The oblique effect of stimulus identification considered with respect to two classes of oblique effects. *Perception* **9**, 37–46.
- Foster, D. H. 1983 Visual discrimination, categorical identification, and categorical rating in brief displays of curved lines: implications for discrete encoding processes. *J. exp. Psychol. (Hum. Percept. Perf.)* **9**, 785–806.
- Foster, D. H. & Bischof, W. F. 1987 Bootstrap variance estimators for the parameters of small-sample sensory-performance functions. *Biol. Cyber.* **57**, 341–347.
- Foster, D. H. & Ferraro, M. 1989 Visual gap and offset discrimination and its relation to categorical identification in brief line-element displays. *J. exp. Psychol. (Hum. Percept. Perf.)* **15**, 771–784.
- Green, D. M. & Swets, J. A. 1966 *Signal detection theory and psychophysics*. New York: Wiley.
- Gurnsey, R. & Browse, R. A. 1987 Micropattern properties and presentation conditions influencing visual texture discrimination. *Percept. Psychophys.* **41**, 239–252.
- Gurnsey, R. & Browse, R. A. 1989 Asymmetries in visual texture discrimination. *Spatial Vis.* **4**, 31–44.

- Hubel, D. H. & Wiesel, T. N. 1968 Receptive fields and functional architecture of monkey striate cortex. *J. Physiol.* **195**, 215–243.
- Ike, E. E., Ruddock, K. H. & Skinner, P. 1987 Visual discrimination of simple geometrical patterns: I. Measurements for multiple element stimuli. *Spatial Vis.* **2**, 13–29.
- Javadnia, A. & Ruddock, K. H. 1988 The limits of parallel processing in the visual discrimination of orientation and magnification. *Spatial Vis.* **3**, 97–114.
- Julesz, B. 1981 Textons, the elements of texture perception, and their interactions. *Nature, Lond.* **290**, 91–97.
- Kennedy, H., Martin, K. A. C., Orban, G. A. & Whitteridge, D. 1985 Receptive field properties of neurones in visual area 1 and visual area 2 in the baboon. *Neuroscience* **14**, 405–415.
- Marendaz, C. & Stivalet, P. 1990 Processing of orientation in early vision. *Perception* **19**, 381.
- Neisser, U. 1967 *Cognitive psychology*. New York: Appleton-Century-Crofts.
- Palmer, S. E. & Hemenway, K. 1978 Orientation and symmetry: effects of multiple, rotational, and near symmetries. *J. exp. Psychol. (Hum. Percept. Perf.)* **4**, 691–702.
- Regan, D. & Beverley, K. I. 1985 Postadaptation orientation discrimination. *J. opt. Soc. Am. A* **2**, 147–155.
- Rose, D. & Blakemore, C. 1974 An analysis of orientation selectivity in the cat's visual cortex. *Expl Brain Res.* **20**, 1–17.
- Rubenstein, B. S. & Sagi, D. 1990 Spatial variability as a limiting factor in texture-discrimination tasks: Implications for performance asymmetries. *J. opt. Soc. Am. A* **7**, 1632–1643.
- Sagi, D. & Julesz, B. 1985 'Where' and 'what' in vision. *Science, Wash.* **228**, 1217–1219.
- Sagi, D. & Julesz, B. 1987 Short-range limitation on detection of feature differences. *Spatial Vis.* **2**, 39–49.
- Stiles, W. S. 1978 *Mechanisms of colour vision*. London: Academic Press.
- Swets, J. A. 1973 The relative operating characteristic in psychology. *Science, Wash.* **182**, 990–1000.
- Thomas, J. P. & Gille, J. 1979 Bandwidths of orientation channels in human vision. *J. opt. Soc. Am.* **69**, 652–660.
- Treisman, A. 1985 Preattentive processing in vision. *Computer Vis. Graphics Image Proc.* **31**, 156–177.
- Treisman, A. & Gormican, S. 1988 Feature analysis in early vision: Evidence from search asymmetries. *Psychol. Rev.* **95**, 15–48.
- Treisman, A. M., Sykes, M. & Gelade, G. 1977 Selective attention and stimulus integration. In *Attention and performance*, vol. 6 (ed. S. Dornic), pp. 333–361. Hillsdale, New Jersey: Lawrence Erlbaum Associates.
- Treisman, A. & Souther, J. 1985 Search asymmetry: A diagnostic for preattentive processing of separable features. *J. Exp. Psychol. (Gen.)* **114**, 285–310.
- Watt, R. J. 1987 Scanning from coarse to fine spatial scales in the human visual system after the onset of a stimulus. *J. opt. Soc. Am. A* **4**, 2006–2021.

Received 17 September 1990; accepted 29 October 1990